Structure and composition of high redshift radio galaxies

Collaborators:

Joël Vernet (ESO)
Montse Villar-Martîn (Sheffield)
Marshall Cohen (Caltech)
Sperello di Serego Alighieri (Arcetri)
Andrea Cimatti (Arcetri)
Laura Pentericci (Leiden)
Pat McCarthy (OCIW)

The programme:

To isolate the different sources of radiation in massive galaxies at early epochs. The galaxies are identified by virtue of their powerful radio emission and studied in the optical, NIR, MIR, FIR, and (sub-)mm bands.

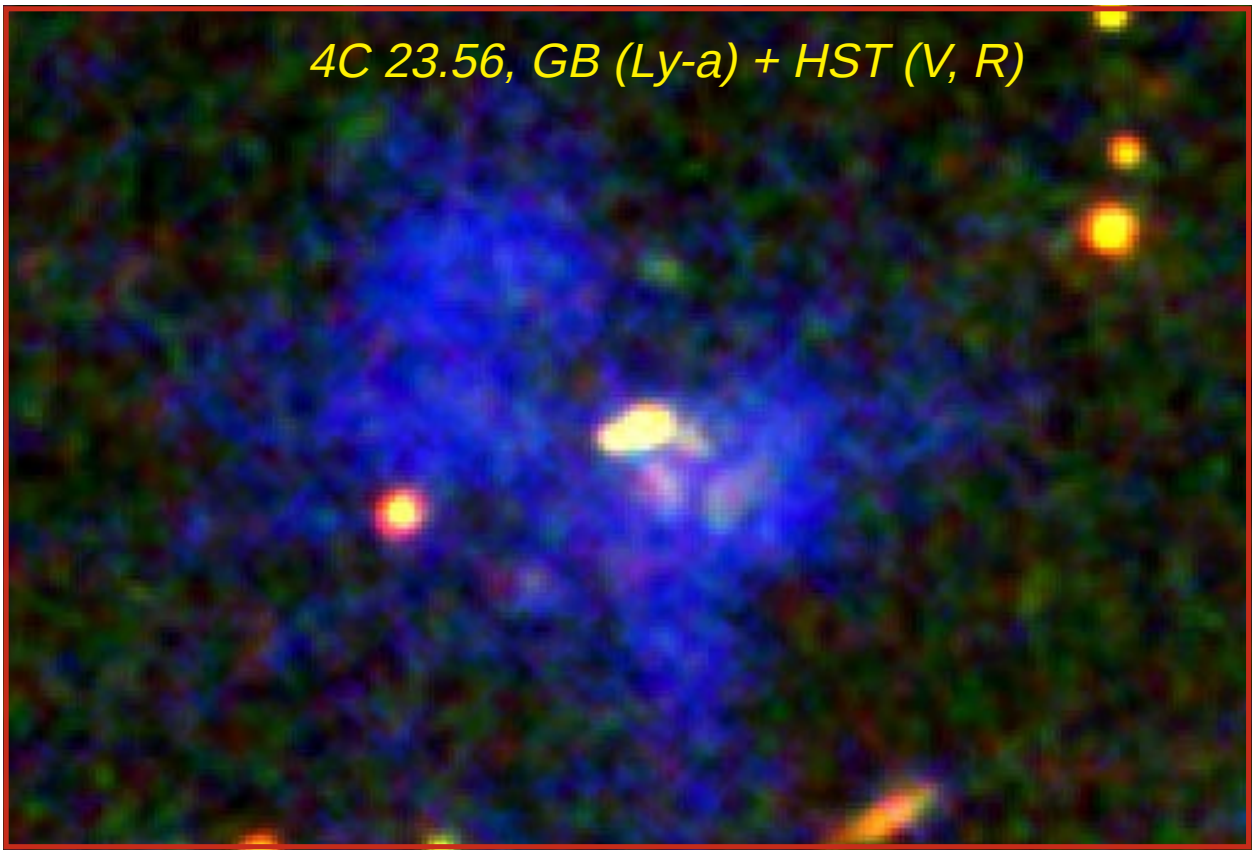

This talk:

Preliminary results from Keck spectropolarimetry and HST imaging of a sample of z ~ 2.5 radio galaxies.

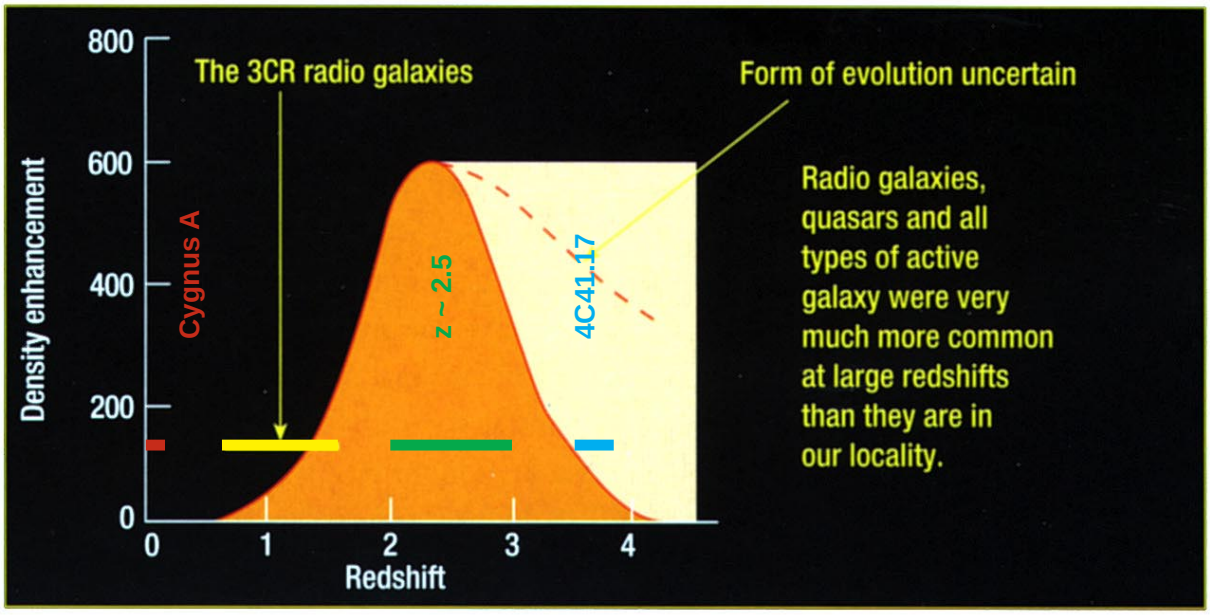

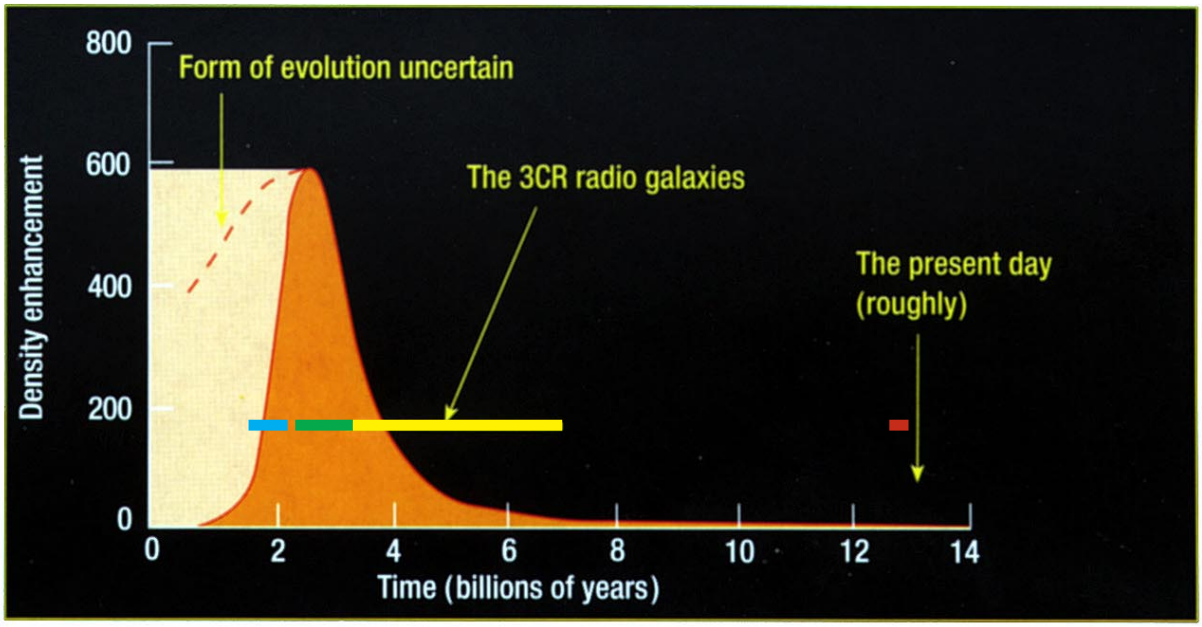

From Longair (1997, A&G, 38, 10)

The sample:

This sample is of RG with z ~ 2.5 which allows us to study the strong UV emission lines from Ly-α -> CIII], the UV continuum, resonance absorption lines and the 2200 Å dust feature — all in the optical band — and to straddle the 4000 Å break in the J -> K bands

Our principal sample constists of six objects with 2.3 < z < 2.9 and this is suplemented by four sources from the literature having similar quality data but extending the redshift range to 1.8 < z < 3.8

The data:

NICMOS and WFPC 2 images give us the morphology in the rest-frame optical and UV, and Keck (LRISp) spectropolarimetry gives us a very powerful tool for disassembling the UV spectral components

Object	z
4C 23.56a	2.482
4C 23.56b	2.482
4C -00.54	2.366
TXS 0211-122	2.338
B3 0731+438	2.429
USS 0828+193	2.572
MRC 0943-242	2.9
4C 41.17	3.798
FSC10214+4724	2.2824
MRC 2025-218	2.63
3C 256	1.824

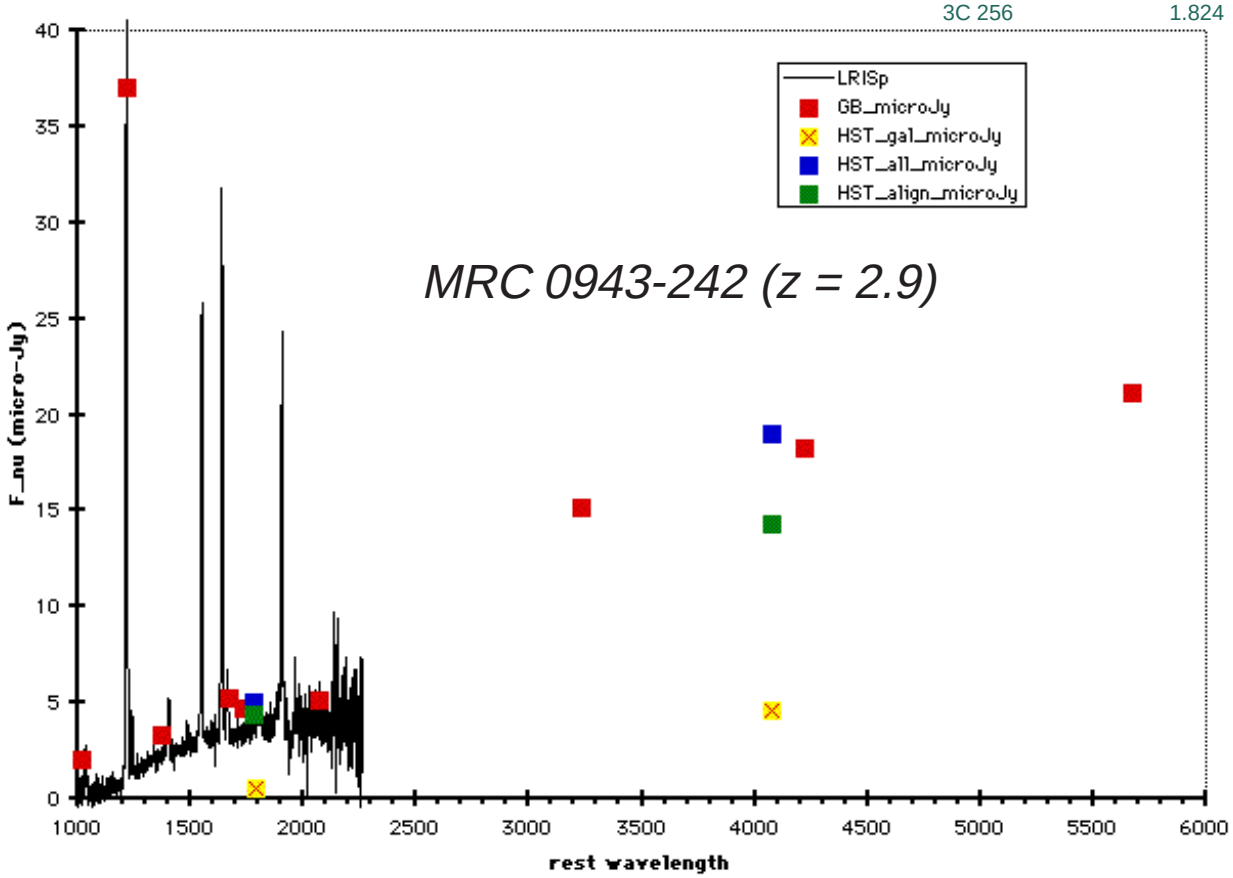

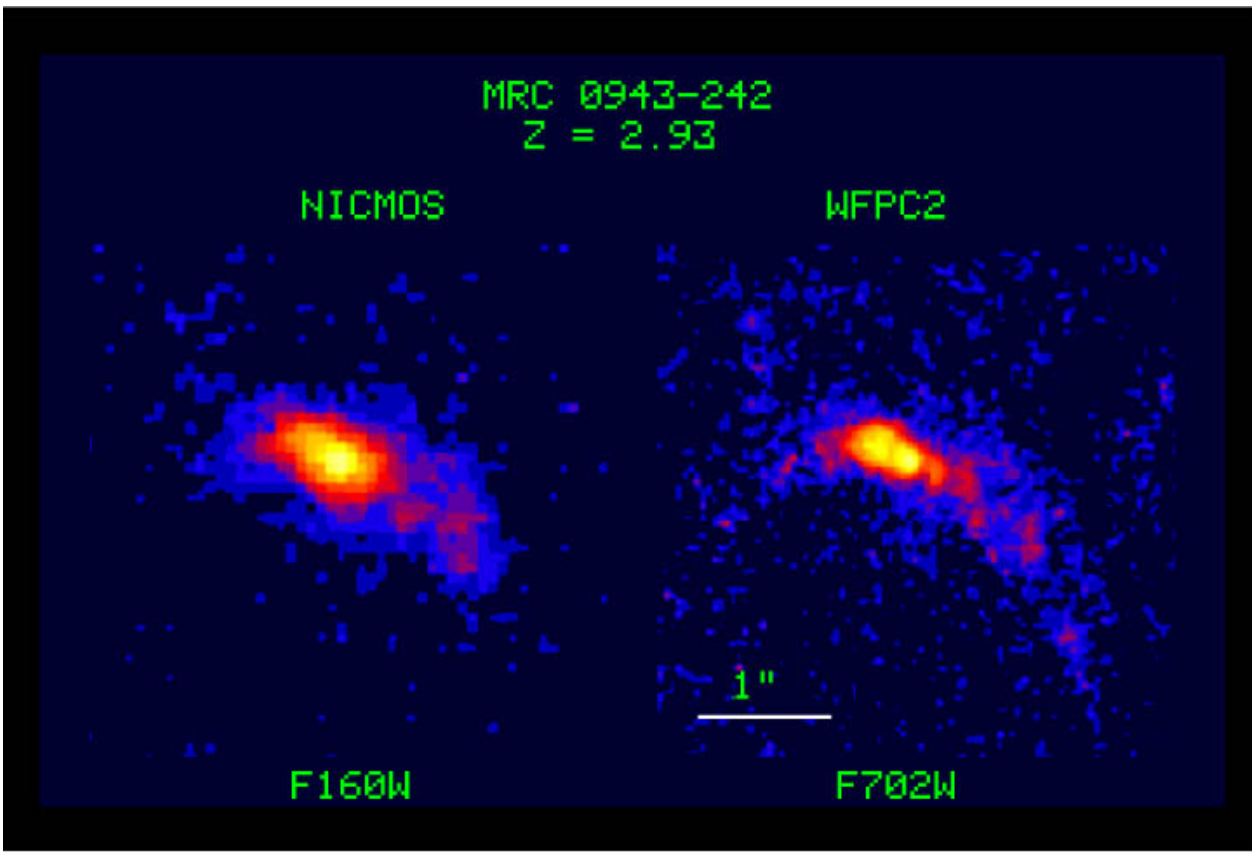
MRC 0943-242
Z = 2.93
NICMOS
WFPC2
1"
F160W
F702W

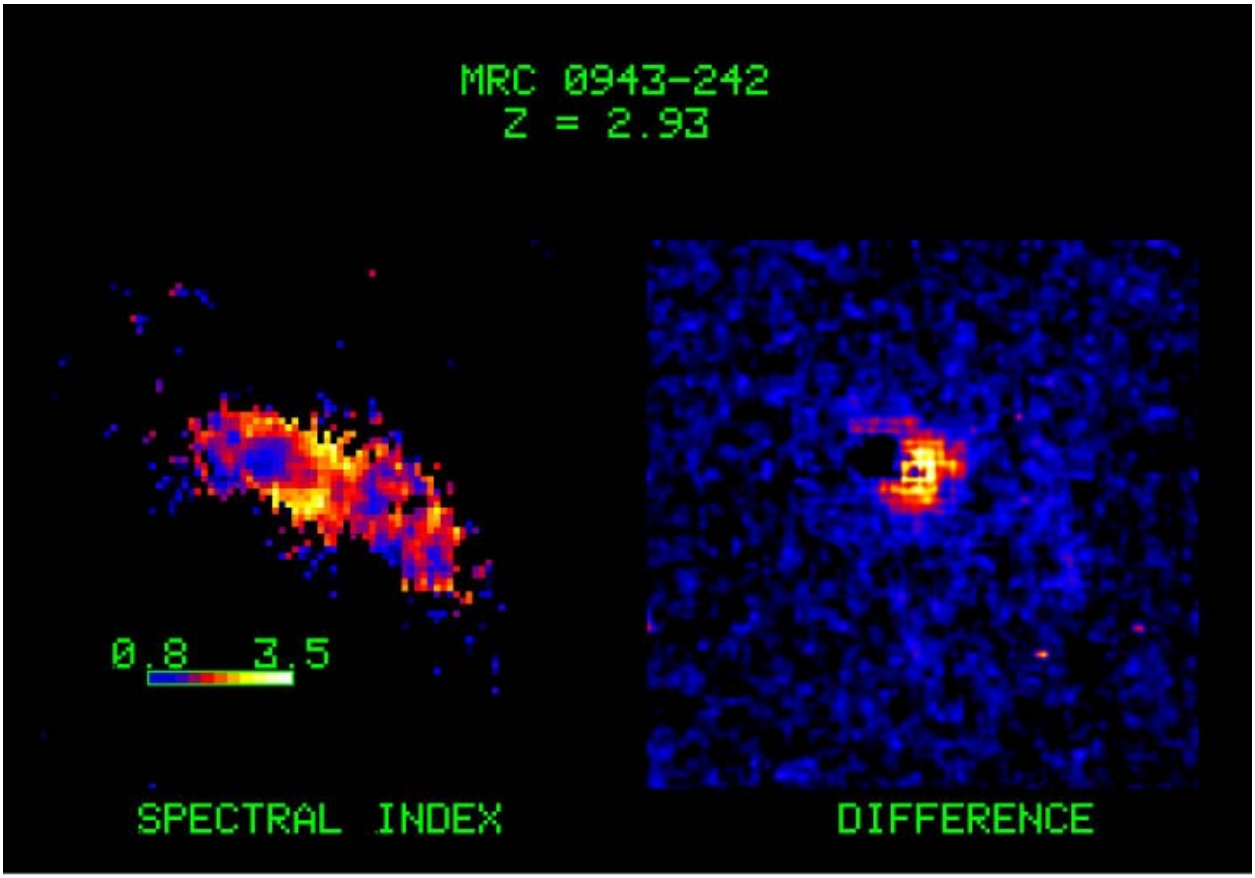
MRC 0943-242
Z = 2.93
0.8
3.5
SPECTRAL INDEX
DIFFERENCE

Principal results:

- All sources show a strong ‘alignment effect’ between their UV and radio morphologies although the structures are complex. One case, 4C 23.56, shows a beautiful ‘ionization cone’ in Ly-α. The brightest UV emission is extended and does not necessarily coincide with the nucleus (radio core)

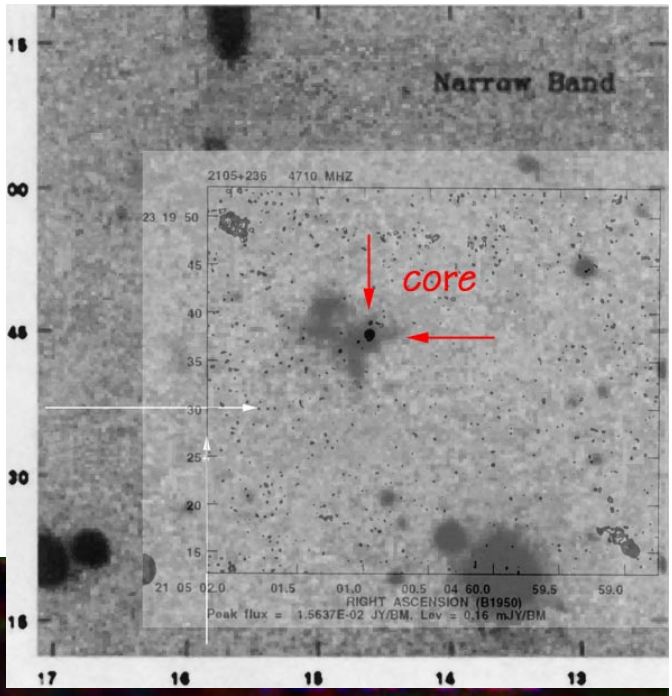

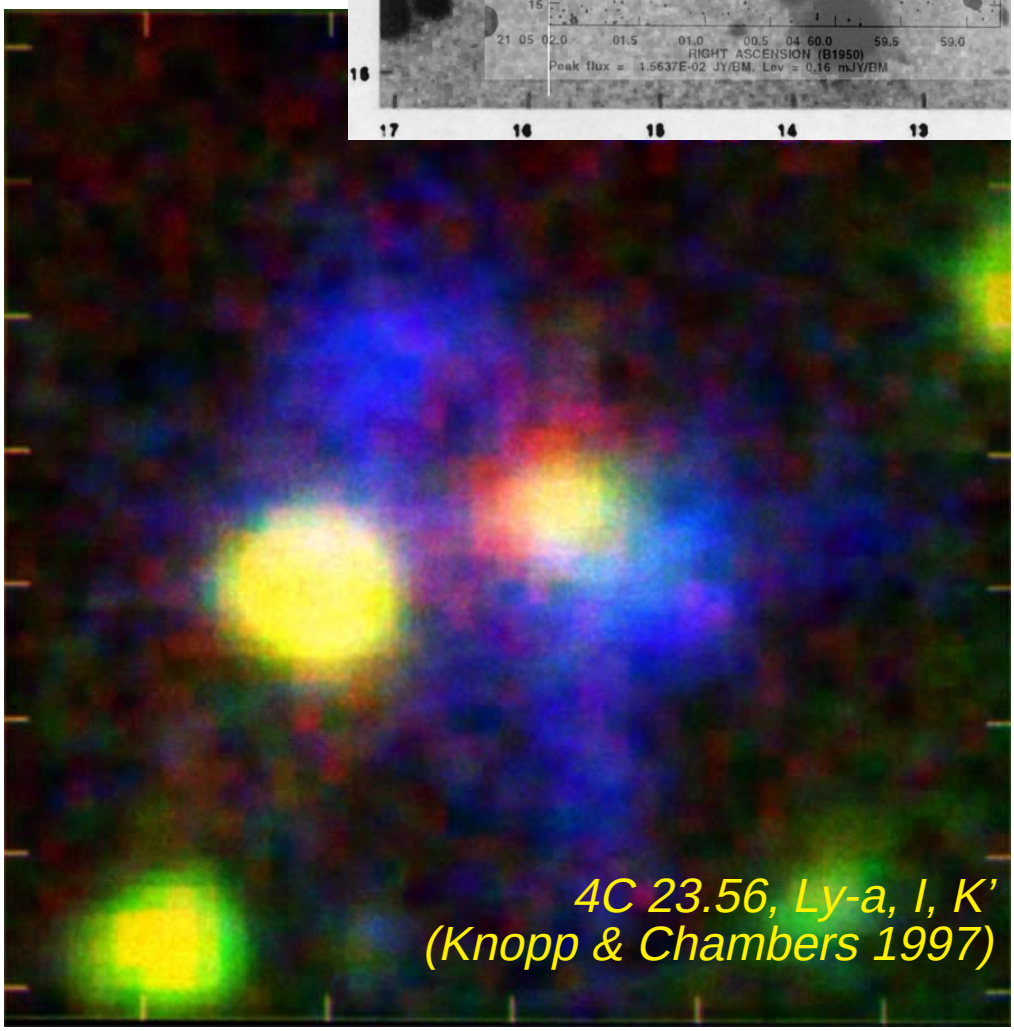

4C 23.56, Ly-a, I, K’
(Knopp & Chambers 1997)

- The continuum colours are remarkably similar and can be fitted by a power law absorbed by a standard Galactic (in the RG rest-frame) extinction law with E(B-V) ~ 0.1 (which corresponds to $\tau \sim 1$ at 1500 Å).

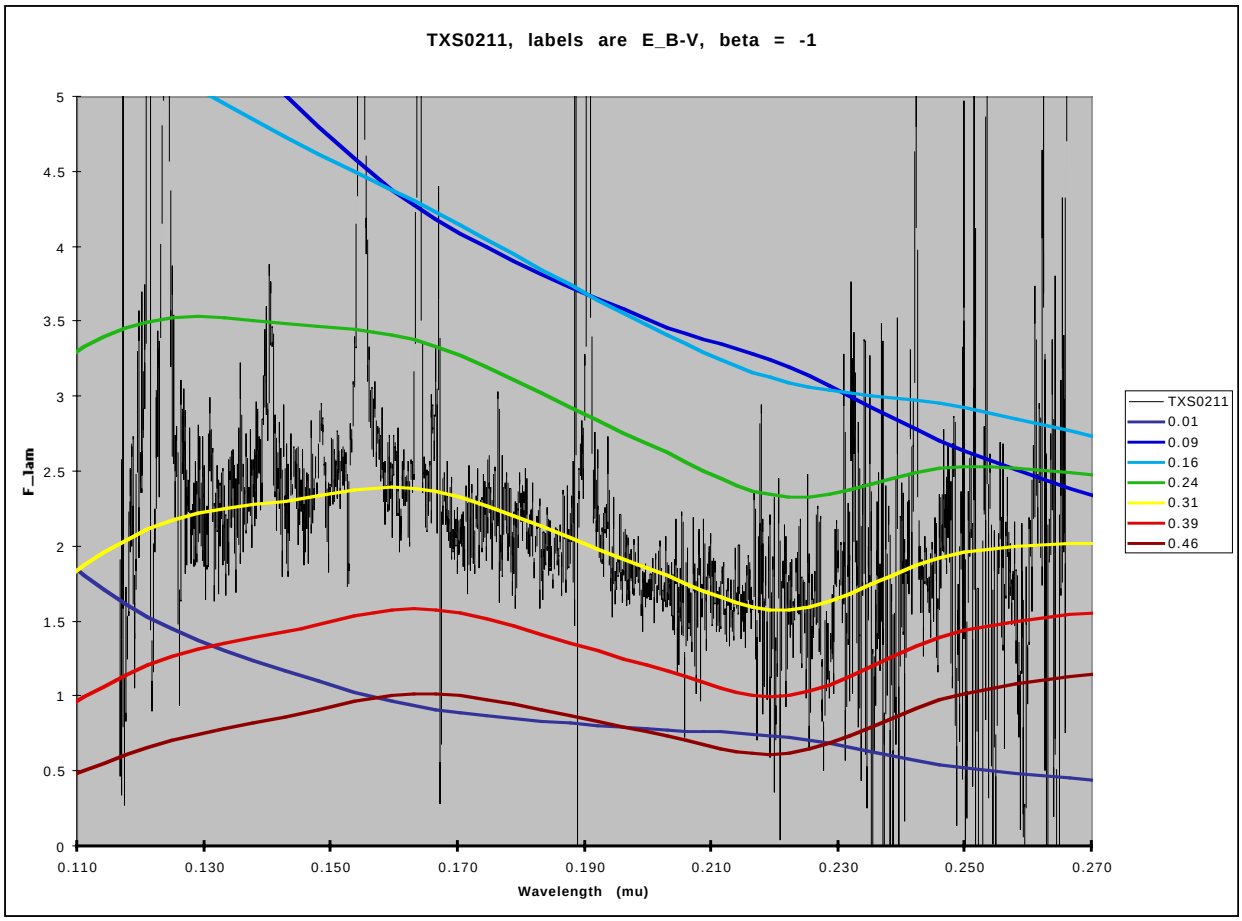

Simple 'scattering atmosphere' model ($\tau\, e^{-\tau}$)

Continuum points and their weights have been isolated in the following spectra and a reddened power law ($f_\lambda \sim \lambda^\beta$) fitted. These are simple 'screen extinction' models.

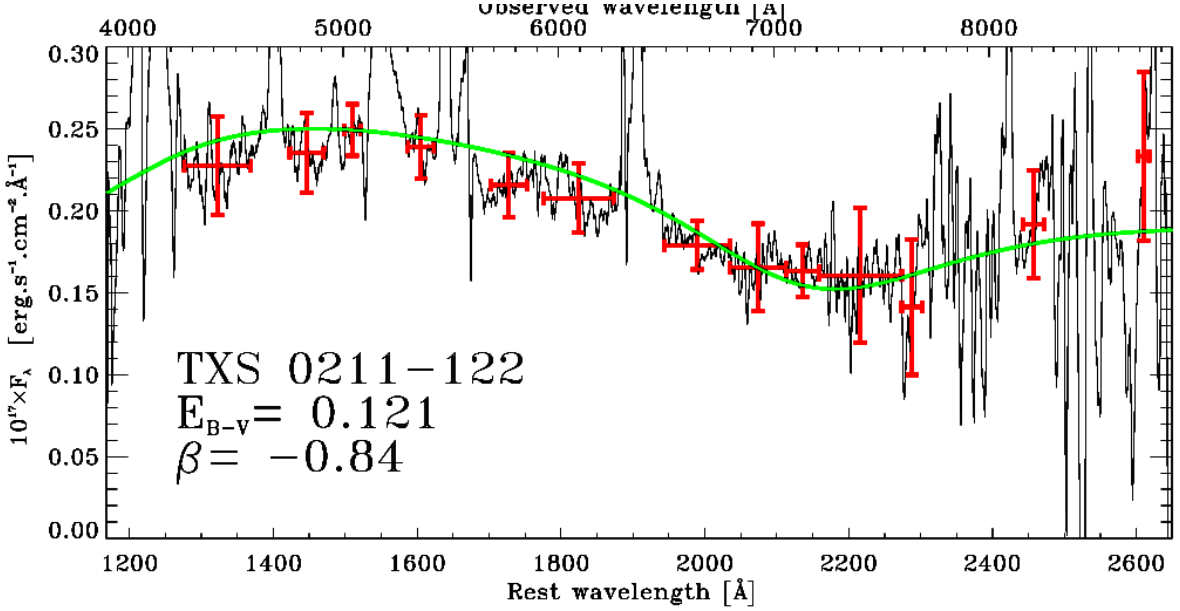
Observed wavelength [Å]
4000
5000
6000
7000
8000
0.30
0.25
0.20
0.15
0.10
0.05
0.00
$10^{17}\times F_\lambda$ [erg.s^{-1}.cm^{-2}.Å^{-1}]
TXS 0211−122
E_{B-V}= 0.121
β= −0.84
1200
1400
1600
1800
2000
2200
2400
2600
Rest wavelength [Å]

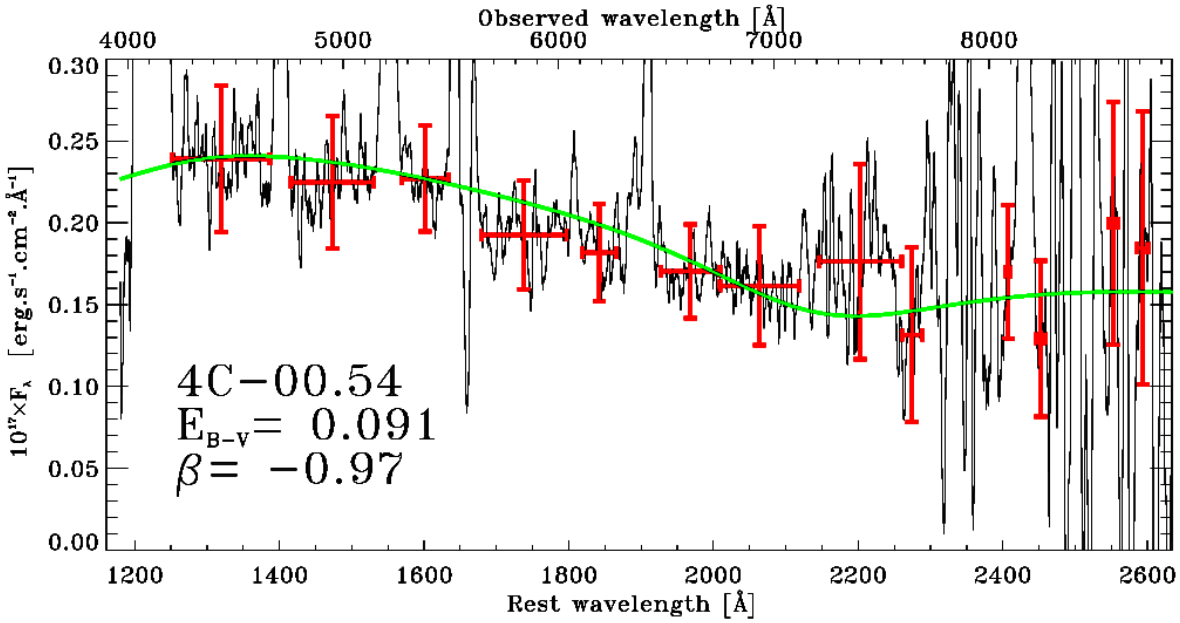
Observed wavelength [Å]
4000
5000
6000
7000
8000
0.30
0.25
0.20
0.15
0.10
0.05
0.00
$10^{17}\times F_\lambda$ [erg.s^{-1}.cm^{-2}.Å^{-1}]
4C−00.54
E_{B-V}= 0.091
β= −0.97
1200
1400
1600
1800
2000
2200
2400
2600
Rest wavelength [Å]

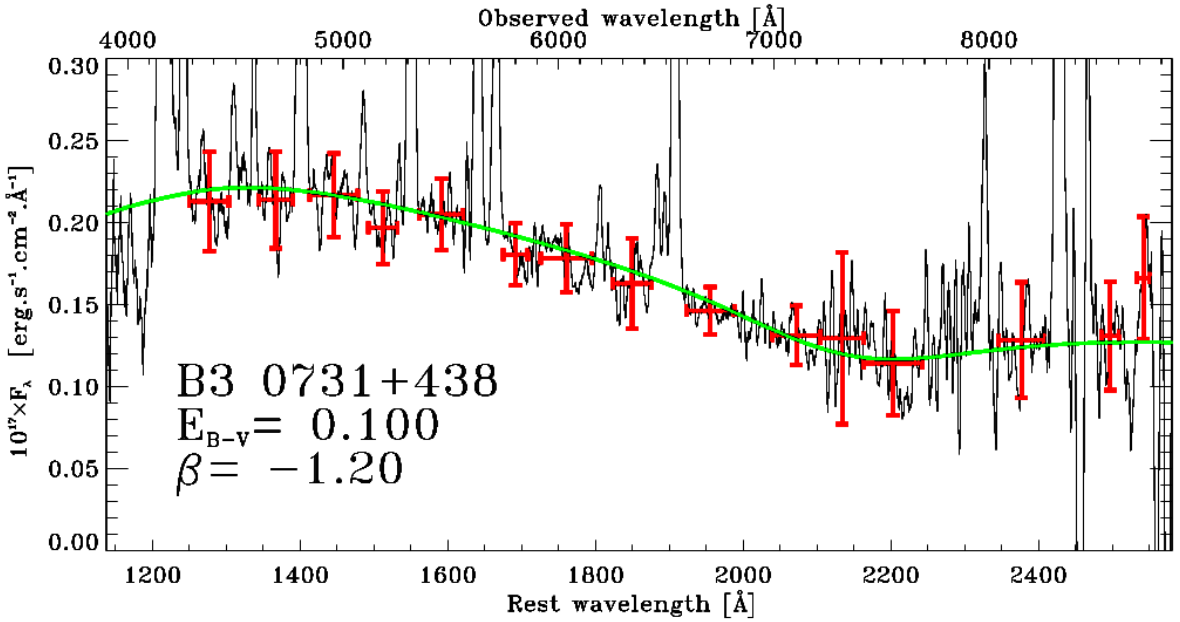
Observed wavelength [Å]
4000
5000
6000
7000
8000
0.30
0.25
0.20
0.15
0.10
0.05
0.00
$10^{17}\times F_\lambda$ [erg.s^{-1}.cm^{-2}.Å^{-1}]
B3 0731+438
E_{B-V}= 0.100
β= −1.20
1200
1400
1600
1800
2000
2200
2400
Rest wavelength [Å]

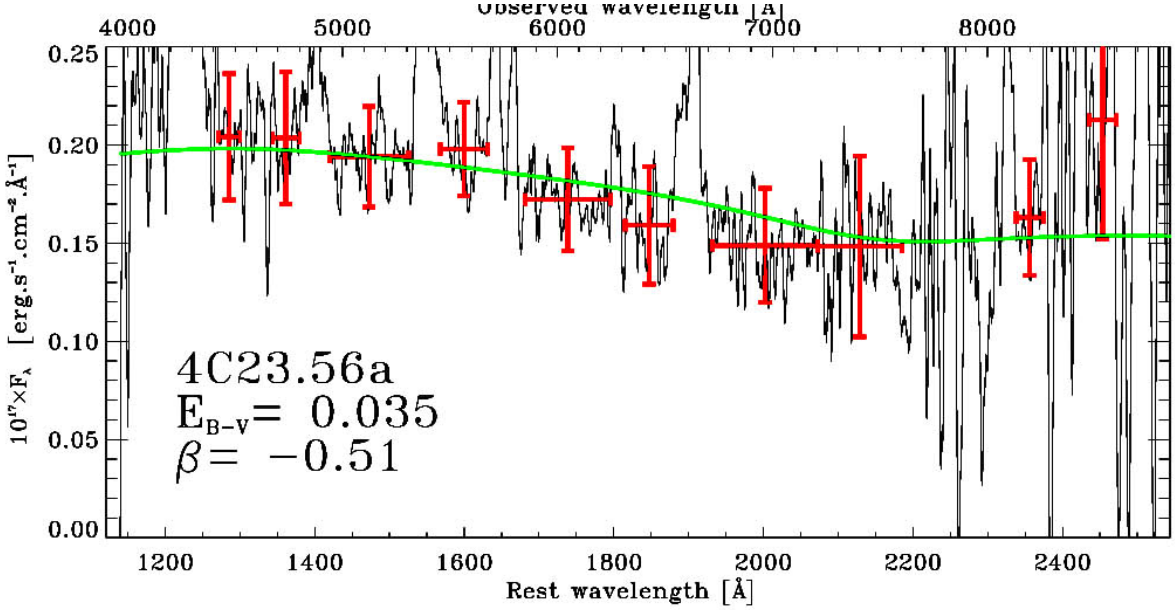
Observed wavelength [Å]
4000
5000
6000
7000
8000
0.25
0.20
0.15
0.10
0.05
0.00
$10^{17}\times F_\lambda$ [erg.s^{-1}.cm^{-2}.Å^{-1}]
4C23.56a
E_{B-V}= 0.035
β= −0.51
1200
1400
1600
1800
2000
2200
2400
Rest wavelength [Å]

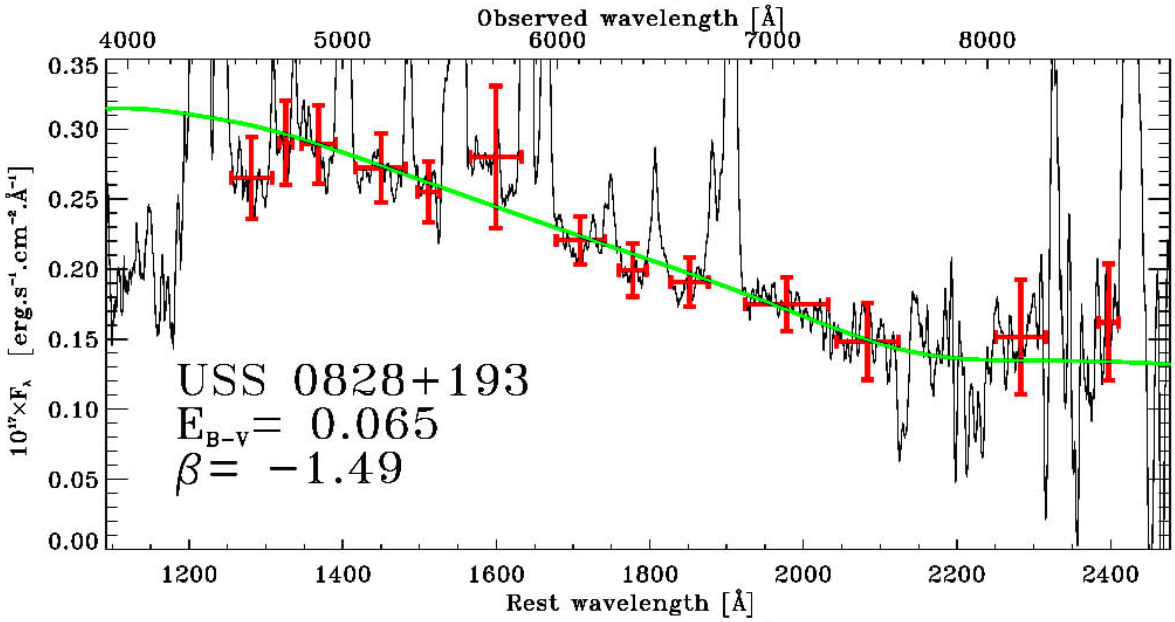
Observed wavelength [Å]
4000
5000
6000
7000
8000
0.35
0.30
0.25
0.20
0.15
0.10
0.05
0.00
$10^{17}\times F_\lambda$ [erg.s^{-1}.cm^{-2}.Å^{-1}]
USS 0828+193
E_{B-V}= 0.065
β= −1.49
1200
1400
1600
1800
2000
2200
2400
Rest wavelength [Å]

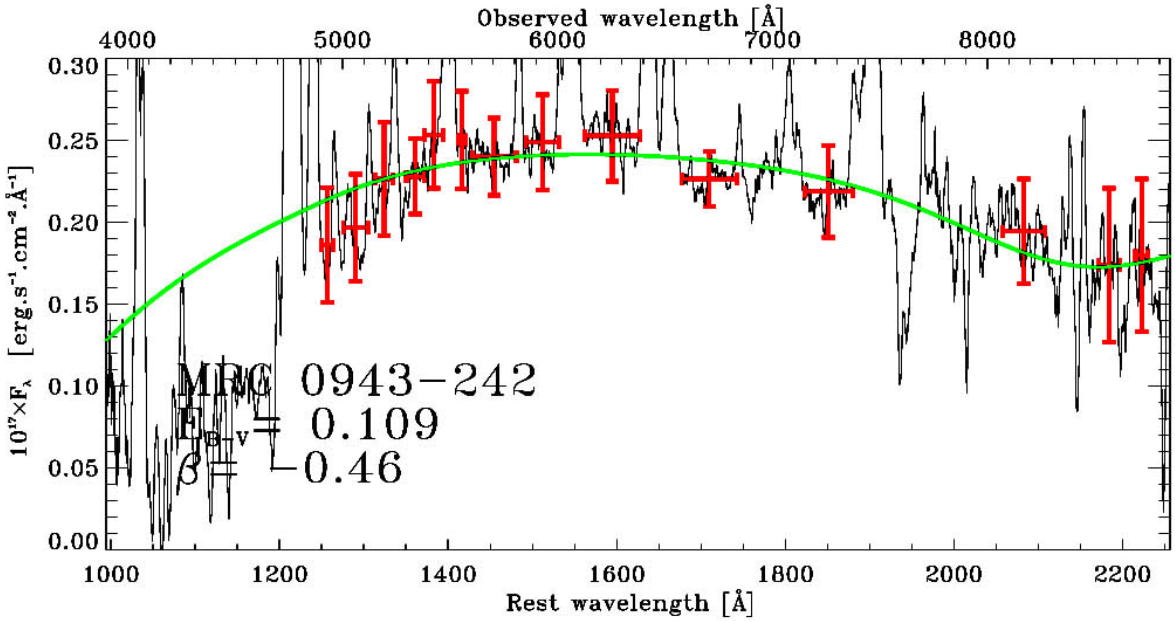
Observed wavelength [Å]
4000
5000
6000
7000
8000
0.30
0.25
0.20
0.15
0.10
0.05
0.00
$10^{17}\times F_\lambda$ [erg.s^{-1}.cm^{-2}.Å^{-1}]
MRC 0943−242
E_{B-V}= 0.109
β= −0.46
1000
1200
1400
1600
1800
2000
2200
Rest wavelength [Å]

- Interstellar absorption lines are seen and, in some objects, there is evidence for wind and photospheric absorption lines from hot stars. Several sources show complex, spatially extended absoption structures at Ly-α
- The emission lines are spatially extended (up to ~ 20 arcsec = 140kpc for Ly-α) and show complex kinematic structures up to ± 2000 km/s

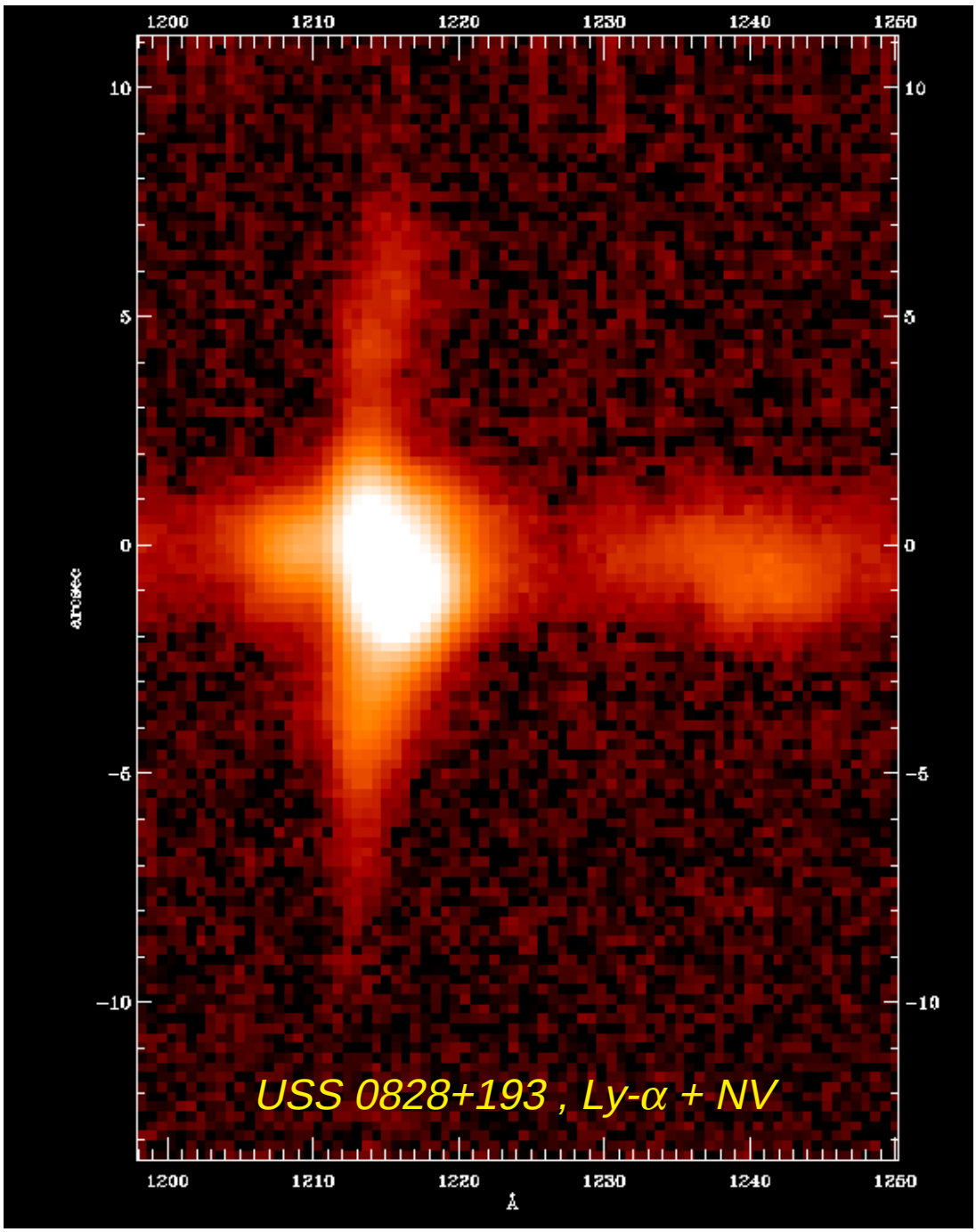

- The continuum linear polarization (measured just longward of Ly-α/NV) ranges from < 3% to > 25%. The E-vector is perpendicular to the UV extension (but not necessarily to the radio axis). HST images are needed to see this

- The emission line spectra indicate a rather constant level of ionization with a small range in the observed CIII]/CIV and HeII/CIV line ratios.

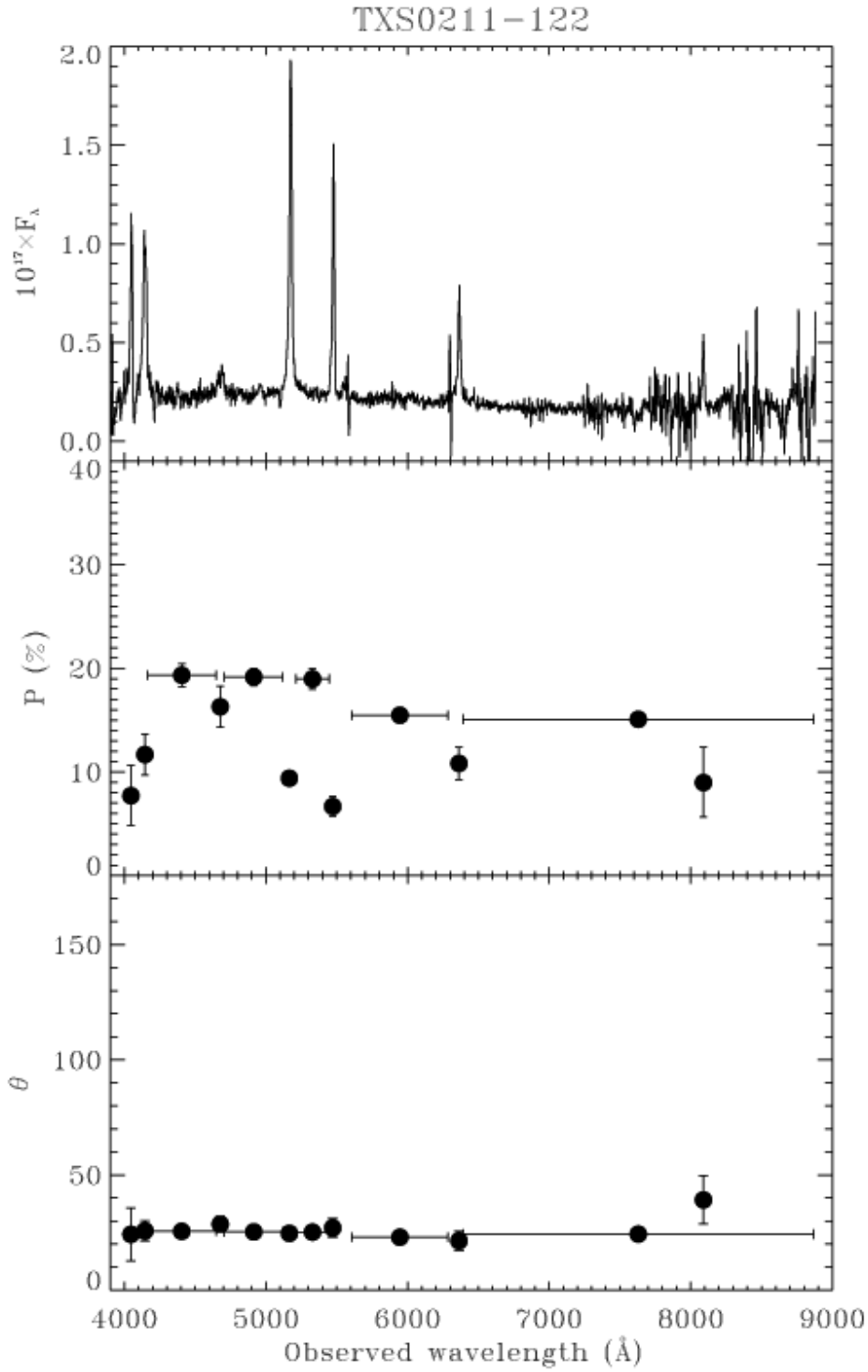

❑ Amongst the spatially integrated properties, the strongest correlations are observed to be:

1) between continuum polarization (P) and the Ly-α/CIV emission line ratio (anticorrelation)

2) between P and the NV/CIV ratio

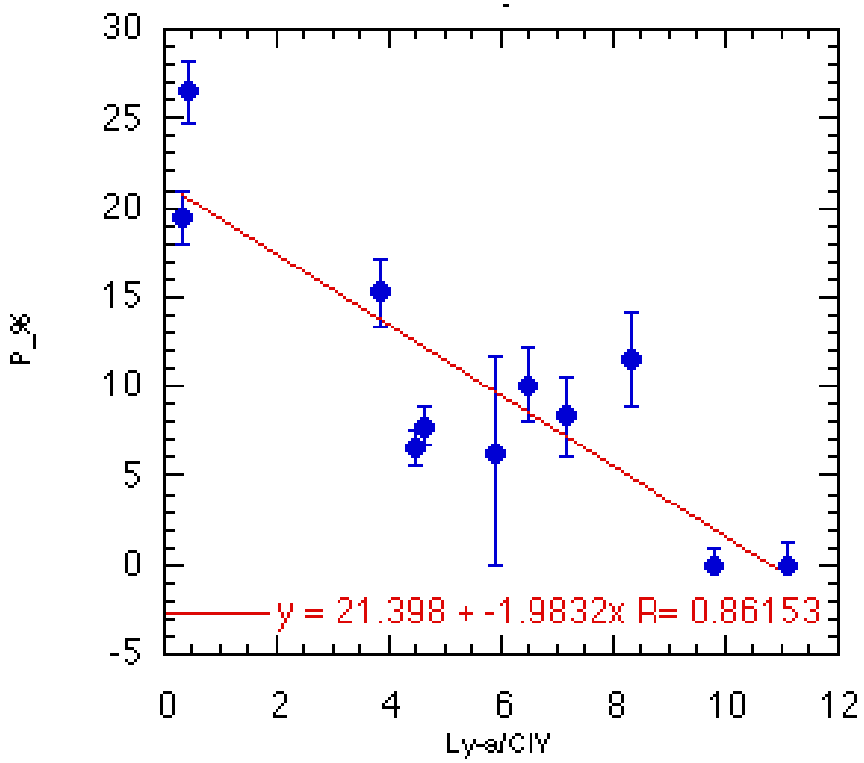

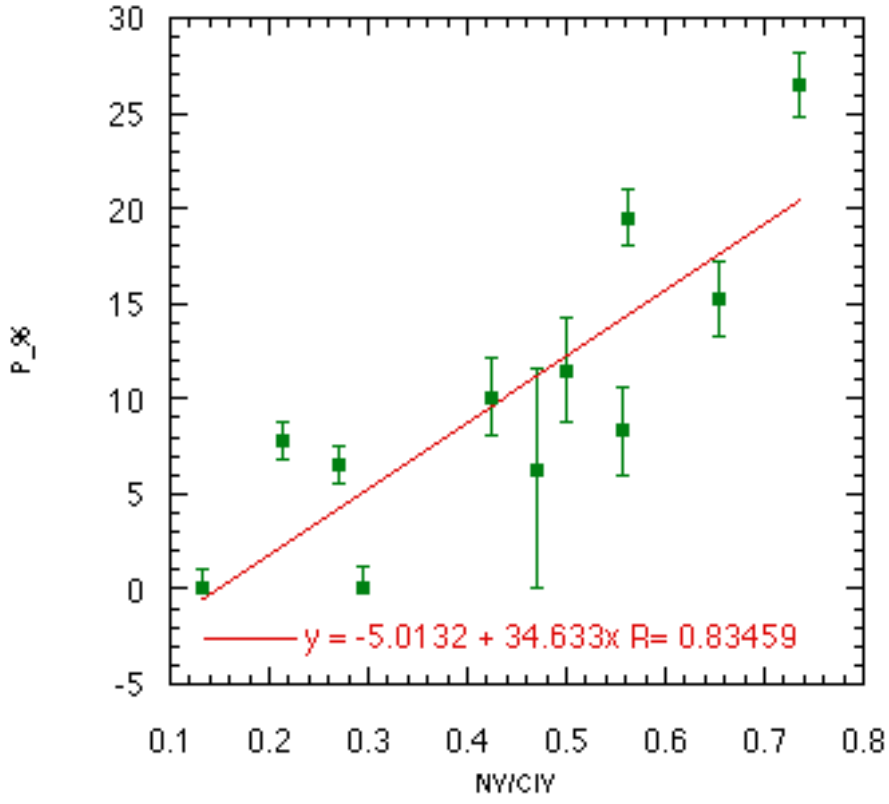

Interpretation:

- ❏ Powerful radio galaxies contain (hidden) QSO nuclei whose EUV emission ionizes the extended gas along the radio axis and whose FUV emission we see scattered by extended dust structures

- ❏ The scattered component can — but may not always — dominate the observed UV continuum and there is evidence for an unpolarized hot stellar component in addition to a (generally small) nebular continuum component

- ❏ There is a direct connection between the scattering mechanism (which produces the polarization) and the destruction of Ly-α

- ❏ The continuua exhibit dust extinction, some of which may be from an extended (not necessarily neutral) halo outside the regios which see the QSO. This dust shows the 2200 Å feature. However, the similarity of the derived reddenings suggests a ‘scattering atmosphere’ mechanism where most of the light we see comes from regions where $\tau \sim 1$

- ❏ There appears to be strong connection between the dominance of scattered light (dust abundance and/or intrinsic quasar luminosity?) and nitrogen/carbon ratio (see Hamann & Ferland (1993) for the nitrogen story in high z QSOs). The behaviour of the NV/CIV, NV/HeII diagram indicates that the effect is due to nitrogen abundance variations and not carbon depletion onto grains

The future:

These objects are telling us the story of the formation of massive galaxies and their quasar nuclei during the epoch when AGN had their maximum space density.

The UV emission lines tell us something about chemical composition of the extended nebulosity but to do the job properly, we need to measure the optical forbidden line spectrum in the IR (VLT/ISAAC).

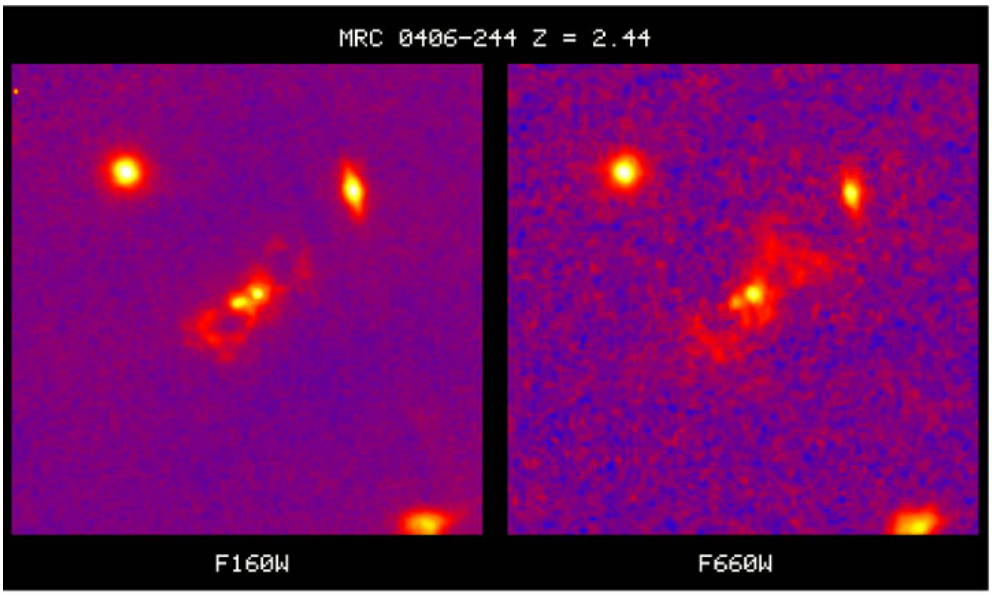

HST, NICMOS + WFPC 2, McCarthy, 1998

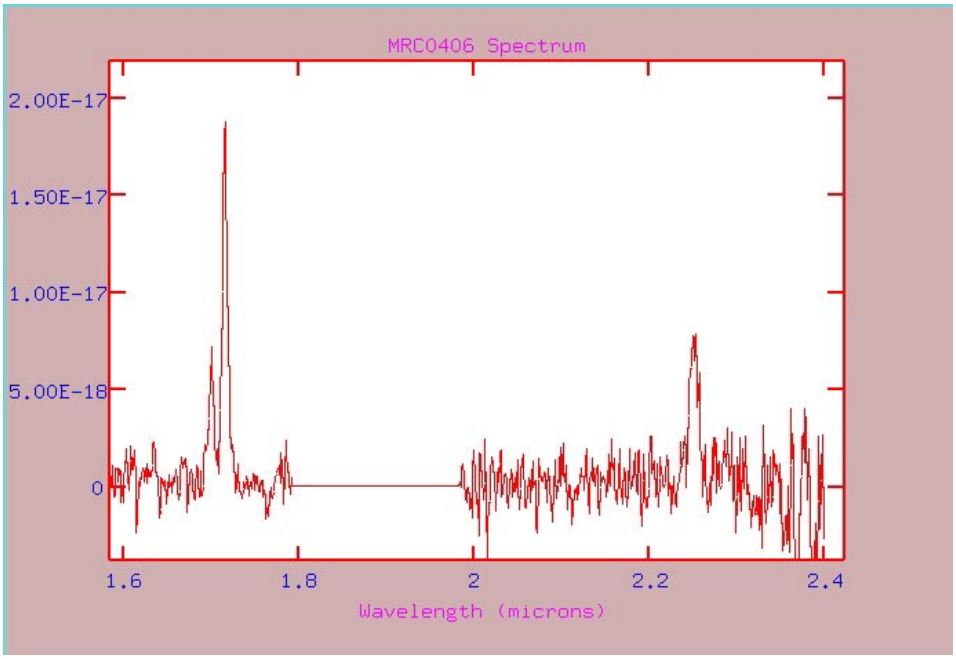

ESO NTT, SOFI, (Moorwood 1998)

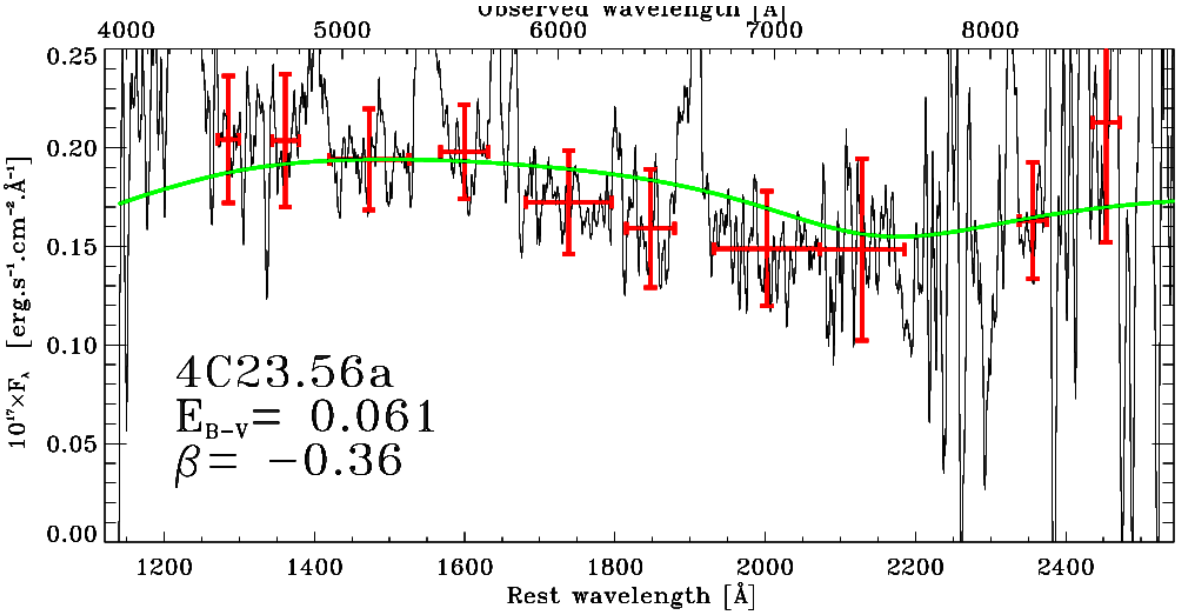

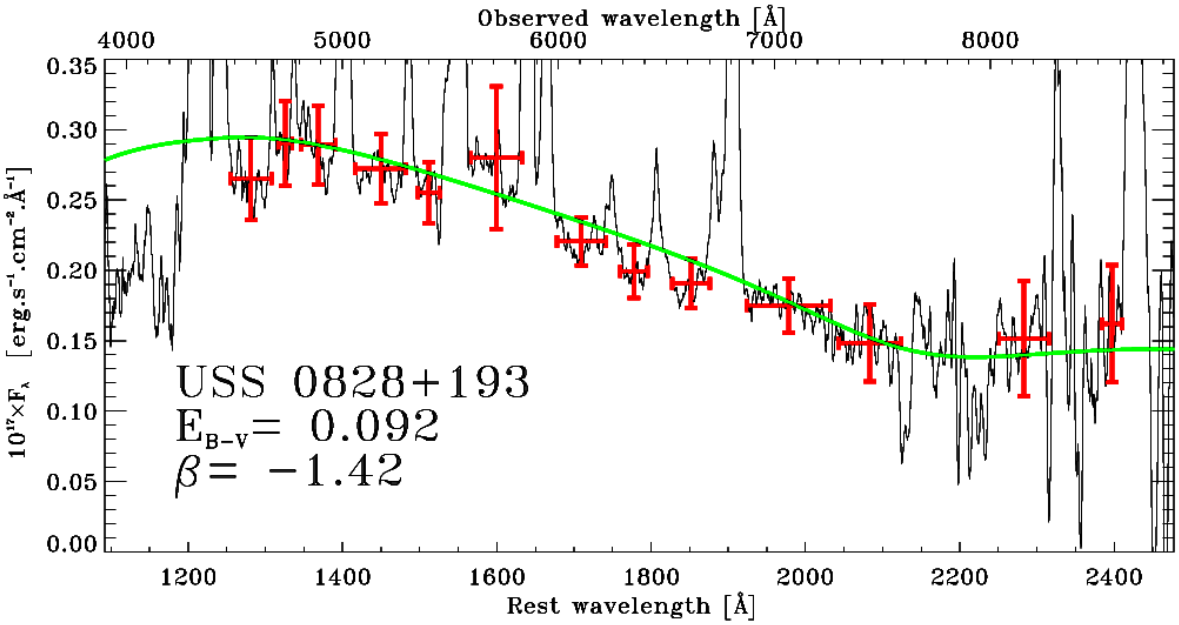

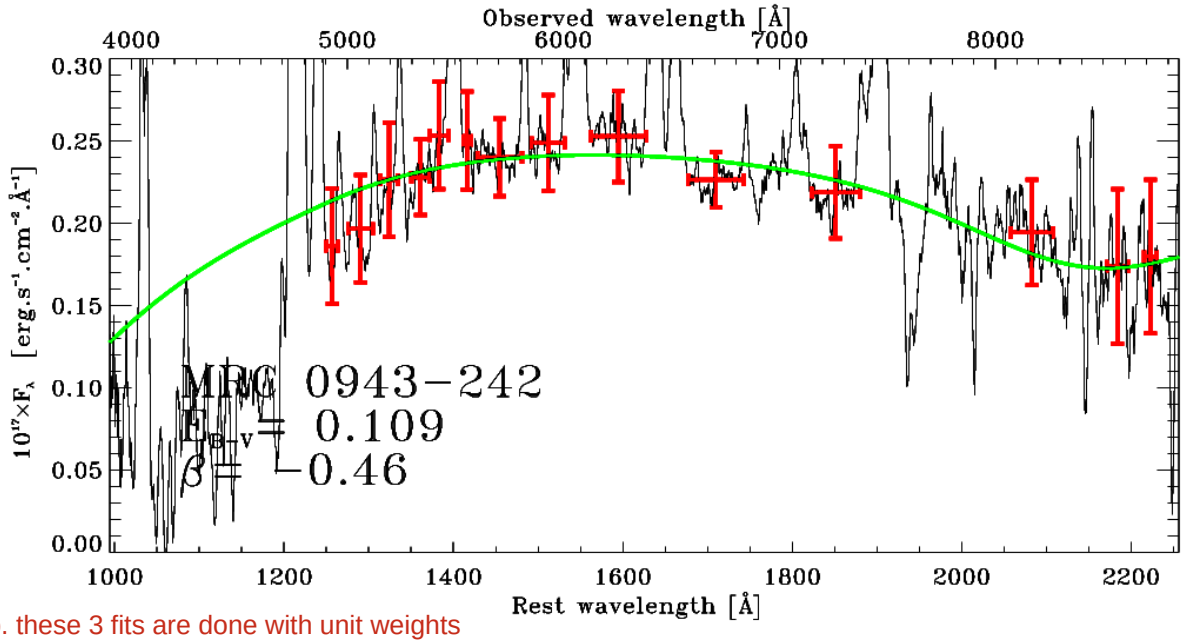

nb. these 3 fits are done with unit weights